

Quasicrystalline Metal Powder: A Potential Filler for UHMWPE Composites

Lucas Ricardo Fernandes Figueiredo^a, Tibério Andrade Passos^a, Angelo Vieira Mendonça^b,

Lucineide Balbino Silva^{**} 

^aUniversidade Federal da Paraíba, Programa de Pós-graduação em Ciência e Engenharia de Materiais, Cidade Universitária, 58051-900, João Pessoa, PB, Brasil.

^bUniversidade Federal da Paraíba, Programa de Pós-graduação em Engenharia Civil e Ambiental, Cidade Universitária, 58051-900, João Pessoa, PB, Brasil.

Received: July 22, 2021; Revised: December 11, 2021; Accepted: December 13, 2021

The mechanical and thermal behavior of ultra-high molecular weight polyethylene (UHMWPE)/metallic quasicrystal powder (MQP) composites are evaluated at filler volume fractions (ϕ_f) of 0.01, 0.02, 0.06 and 0.15. MQP is based on an aluminum alloy, synthesized and characterized to act as a filler for UHMWPE. The preparation of the composites was conducted by compression molding. Morphological analysis reveals larger and smaller MQP particles, being well distributed, and mechanically anchored in the matrix. The melting temperature was maintained after adding filler, while the crystallinity values decreased. When adding MQP, an improvement in thermal stability is observed by increases in both the initial and maximum weight loss rate temperatures (T_{max}). However, when the temperature is about 700°C all composites present oxidation due to the MQP presence. The Pukansky model shows that the 0.06 MQP composites have better interfacial adhesion. This is confirmed by the Nicolais-Narkis equation. This contributes to an increase in the modulus of elasticity of the 0.06 MQP composite in respect to the others. The elongation at break was reduced for the 0.15 MQP composite. However, the higher volume fraction of MQP increased the stiffness of the UHMWPE, reflecting its potential for use as a reinforcement.

Keywords: UHMWPE, composite, metallic quasicrystal, Pukánszky's Model.

1. Introduction

Ultra-High Molecular Mass Polyethylene (UHMWPE) presents attractive properties, including biocompatibility, chemical resistance, durability, low friction coefficients, and excellent self-lubrication^{1,2}. In addition, UHMWPE has been used in a variety of applications, from medical implants to industrial and aerospace machines. Yet UHMWPE presents certain drawbacks in respect to elastic modulus, surface hardness, wear resistance and thermal deformation temperatures, as well as poor processing characteristics³⁻⁵. Some researchers have investigated the addition of inorganic particles to UHMWPE (and other polymeric matrices), seeking to improve their mechanical properties, such as mechanical rigidity, resistance to wear, and to reduce their friction coefficients⁶⁻¹⁰.

It should be noted that MQP is a metallic alloy presenting a quasi-periodic crystalline structure. MQP was first discovered by Shechtman et al.¹¹, and afterwards Levine and Steinhardt¹² classified it as an intermetallic compound without translational periodicity; a new class of ordered structures. MQP also absorbs light, has reduced friction, adhesion and good insulating properties^{13,14}. In contrast, its fragility limits mass applications, and therefore, it has been further explored for surface coatings applications, especially those based on aluminum, where it improves hardness and

anti-adhesion¹⁵. Quasicrystalline particles have also been reported as promising for application in aluminum based metal matrix composites¹⁶.

When considering structural applications for polymeric composites, it is important to account for the load-bearing capacity of the dispersed component, which depends on both particle characteristics and interfacial adhesion. When particulate filled composites fail, and if a coupling agent has not been added between the components, the first step is very frequently the interfacial debonding¹⁷⁻²⁰. Pukánszky¹⁷ has proposed a model to determine a parameter "B" that expresses the filler load-bearing capacity in particulate composites. Studies on the mechanical properties of polymer composites with quasicrystalline metallic fillers are still scarce. Some authors^{21,22} have focused on morphological aspects and thermal behavior. The representation of interfacial interaction of composites by mathematical models are well-documented for many types of filler (CaCO₃, SiO₂, corn cob, calcined mollusk shell waste)¹⁷⁻²⁰. However, for quasicrystalline metallic polymer composites, there are no publications in the current literature involving interfacial interaction studies with compositions from mathematical models. In addition, a high cost/benefit ratio is expected for UHMWPE/quasicrystalline filler composites because in this work the metallic filler is used without surface chemical modification. Other filler types, for example calcined mollusk shell waste¹⁹ need to

*e-mail: lucineide@ct.ufpb.br

be modified in order to improve the properties of recycled Polypropylene composites.

The aim of this work was to evaluate changes in the morphological, thermal, and mechanical behavior of UHMWPE promoted by additions of different aluminum alloy contents based on MQP. In addition, this work also intends to predict interfacial interaction in the UHMWPE/MQP composites in uniaxial tensile testing with the application of mathematical approaches based on the Pukánszky Model¹⁷ and Nicolais-Narkis equation²³.

2. Experimental

2.1. Materials

The commercial UHMWPE powder (UTEC 3041) investigated in this study was supplied by Braskem at $M_w = 6 \times 10^6 \text{ g.mol}^{-1}$, which was used as received. The $\text{Al}_{65}\text{Cu}_{23}\text{Fe}_{12}$ icosahedral metallic quasicrystal powder (MQP) was produced in our laboratory. The UHMWPE/MQP composites were prepared at 4.51, 9.02, 22.55 and 45.10 - MQP wt%. Using Equation 1, the MQP volume fraction (\varnothing_f) was calculated as follows:

$$\varnothing_f = \frac{\left(\frac{W_{MQP}}{\rho_{MQP}} \right)}{\frac{W_{MQP}}{\rho_{MQP}} + \frac{W_{UHMWPE}}{\rho_{UHMWPE}}} \quad (1)$$

where W and ρ are the mass and density of the components, and the UHMWPE and MQP densities were 0.951^{24} and 4.51 g.cm^{-125} , respectively.

2.2. Preparation of the samples

Metallic quasicrystal powder: alloy was produced with ingots of Aluminum (99.97% purity), electrolytic copper (99.98% purity), and iron (99.98% purity). The $\text{Al}_{65}\text{Cu}_{23}\text{Fe}_{12}$ alloy (% atomic) was studied by Passos et al.²⁵ due to the low cost of the elements. The elements were melted in an induction furnace with argon atmosphere. After melting, the alloy ingot was then thermally treated under a helium atmosphere at $720 \text{ }^\circ\text{C}$ for 24h. The quasicrystalline alloy obtained was in spherical form and was ground in a planetary mill with a 10:1 sphere/powder ratio for 20 minutes. The particle size of the MQP powder was classified using a 200 sieve mesh (74 microns). The UHMWPE matrix and MQP powder were mechanically mixed for 10 min at room temperature, with several MQP volume fractions obtained by Equation 1 (0.01, 0.02, 0.06 and 0.15); producing homogeneous compositions. The composites were molded by compression molding at a temperature of $200 \text{ }^\circ\text{C}$, pressure of 12 tons using a Marconi hydraulic press. Initially, the sample were pressed by applying 3 tons for 3 minutes. The pressure was then reduced to zero to allow any air that might be trapped in the mold to escape, then 12 tons was applied for 20 minutes. Later, in the final step of molding, the hydraulic press was opened and 25 minutes later, room temperature was reached. The sample was then demolded from the mold to a shape specified by ASTM D 638.

2.3. Characterizations of the samples

Metallic quasicrystal powder (MQP): a) Chemical composition was analyzed by X-ray fluorescence using XRF-1800 Shimadzu equipment at 31.9° ; 40kW; and at 95 milliamps using rhodium X-ray generation; b) Structural composition was determined by X-ray diffraction (XRD) using a Siemens D500 Diffractometer equipped with a (1.54\AA) copper tube at a scan rate of $0.003^\circ.\text{s}^{-1}$ and an angle range between 20 and 50° ; and c) particle size distribution was investigated by laser diffraction using a Cilas laser diffraction analyzer in dry mode.

2.4. Scanning Electron Microscopy (SEM)

The pure polymer and composites morphologies were investigated in a ZEISS LEO 1430 scanning electron microscope. MQP dispersion and interfacial adhesion in the UHMWPE matrix were investigated. The composites molded by compression were immersed in liquid nitrogen and after a few minutes were fractured cryogenically, and then covered with a thin layer of gold for further fracture surface analysis.

2.5. Differential Scanning Calorimetry (DSC)

Thermograms of the composites were obtained using a Shimadzu DSC 60 calorimeter. Calibration used indium and sapphire in the temperature range from 0 to $350 \text{ }^\circ\text{C}$. The sample weights were from 3.0 to 5.0 mg . For each test, the sample was first heated to $200 \text{ }^\circ\text{C}$ at $10 \text{ }^\circ\text{C}.\text{min}^{-1}$ for 3 min, and subsequently cooled down to $30 \text{ }^\circ\text{C}$ at a cooling rate of $10 \text{ }^\circ\text{C}.\text{min}^{-1}$ for data collection. In the second heating scan, the sample was heated from 25 to $200 \text{ }^\circ\text{C}$ at $10 \text{ }^\circ\text{C}.\text{min}^{-1}$ in a nitrogen atmosphere. The crystallization temperature (T_c) was determined during cooling. The melting temperature (T_m) was determined from a second heating scan and the peak area was used to determine the melting enthalpy with constant integration limits. The average temperature values are the average of three measurements. The degree of crystallinity (X_c) was determined using the Equation 2:

$$X_c (\%) = \frac{\Delta H_m}{(1 - W_f) \cdot \Delta H_{100\%}} \cdot 100 \quad (2)$$

where: ΔH_m is the melting enthalpy per unit weight of UHMWPE in the composition, W_f is the weight fraction of quasicrystal powder in the composite, and $\Delta H_{100\%}$ is the enthalpy per unit weight of 100% crystalline polyethylene, which is assumed to be 291 J.g^{-124} .

2.6. Thermogravimetric Analysis (TGA)

The TGA weight loss curves were obtained in a Shimadzu DTG-60H Simultaneous DTA-TG apparatus. Samples of 10 to 11 mg were placed in the equipment oven and heated in a temperature range from 25 to $1000 \text{ }^\circ\text{C}$ at $10 \text{ }^\circ\text{C}.\text{min}^{-1}$ in an Argon (99.99%) atmosphere at $50 \text{ mL}.\text{min}^{-1}$.

2.7. Mechanical properties

Tensile tests were carried out using a universal testing machine, Shimadzu model AG-X 10KN according to ASTM D 638 at an extension rate of $50 \text{ mm}.\text{min}^{-1}$. Five samples were tested for each composite, and mean values were considered.

2.8. Theoretical - calculation of adhesion parameter

The interfacial interaction between filler and matrix is an important factor affecting the mechanical properties of composites. The theoretical tensile strengths of the composites were modeled for adhesion (or not) using (respectively) the Pukánszky and Nicolais-Narkis models^{17,23}.

Based on the Nicolais-Narkis model²³, the applied load is sustained only by the polymer, where the yield strength of the composite should decrease with increasing filler concentration. Yield stress data are obtained from the Equation 3:

$$\frac{\sigma_c}{\sigma_m} = \left(1 - K\phi_f^{\frac{2}{3}} \right) \quad (3)$$

where ϕ_f , σ_c , and σ_m are the respective filler volume fraction, yield stress of the composites, and the matrix. The parameter "K" indicates the extent of adhesion between the filler and the polymer. So, two conditions are evaluable by²³: one considers that $K = 0$, indicating perfect adhesion, and the other that $K = 1.21$, which means no adhesion.

The Pukánszky Model¹⁷ describes composition and interfacial interaction effects on particulate composite yield stress

$$\frac{\sigma_{yc}}{\sigma_{ym}} = \frac{1 + \phi_f}{1 + 2.5\phi_f} \exp(B\phi_f) \quad (4)$$

where σ_{yc} and σ_{ym} are respectively the composite and matrix tensile yield stresses, ϕ_f is the filler volume fraction, and "B" is a parameter which defines the interfacial interaction between the filler and polymer.

In Equation 4, according to B. Pukánszky¹⁷, the first term is related to decreases in the effective capacity of the cross section to support loads; the second term characterizes the interfacial interaction in the composite. The third term associates the area of the interphase with the strength of the interaction, as follows according to Equation 5:

$$B = \left(1 + A_f \rho_f l \right) \ln \left(\frac{\sigma_{yi}}{\sigma_{ym}} \right) \quad (5)$$

where A_f , ρ_f and l are the specific surface area, the filler density, and the thickness of the interface; σ_{yi} is the strength of interaction.

According to Pukánszky et al.^{26,27}, a new equation deduces the reduced yield stress (σ_{yred}), as shown in Equation 6, and eliminates the effect of the reduced load-bearing capacity in the cross section; from Equation 5, A_f , ρ_f are held constant:

$$\sigma_{yred} = \frac{\sigma_{yc} (1 + 2.5\phi_f)}{(1 - \phi_f)} = \ln \sigma_{ym} + B\phi \quad (6)$$

Equation 6 is plotted against the filler content in a linearized version of Equation 4 to obtain the "B" parameter from the straight line slope, whose value reflects the polymer-filler adhesion strength.

3. Results and Discussions

3.1. Structure of the metallic quasicrystal powder

MQP alloy preparation was performed using two melting procedures, one for initial melt and the other upon re-melting. Both processes were conducted using an induction furnace. Figure 1a shows the XRD pattern of MQP that was not thermally treated and the Figure 1b presents the second sample after thermal treatment. The sample without thermal treatment corresponds to the non-quasicrystalline phase (β) and the second thermally treated sample refers to the icosahedral phase (Ψ)²⁵. The composition of the heat treated MQP obtained by X-ray fluorescence is shown in Table 1. The MQP component values are close to the theoretical composition, namely 65% Al, 23% Cu, and 12% Fe ($Al_{65}Cu_{23}Fe_{12}$)²⁸. For the non-thermally treated MQP sample (Figure 1a), both the icosahedral phase (Ψ) and the non-quasicrystalline phase (β) are observed in the diffractogram. J. M. Dubois²⁹ observed a considerable increase in the icosahedral phase (Ψ), which was produced using an AlCuFe alloy under thermal treatments. This result was attributed to peritectic transformations. A icosahedral phase - phase (β) mixture was formed by mechanical alloying of ingots of Al, Cu and Fe, even after vacuum annealing at around 600 °C^{30,31}. In the present work, the MQP was treated for 24h under vacuum at 720 °C, resulting in both the icosahedral phase (Ψ) and the (β)-phase, as shown in Figure 1b.

3.2. Particle size distribution of the metallic quasicrystal powder

The particle size distribution of the thermally treated sample is shown in Figure 2. A wider particle size distribution was verified for the MQP powder, with average diameter of 13.03 μm . The cumulative distribution indicates that 10% of the particles present diameter below 1.81 μm and that 50% have a diameter below 8.51 μm . In addition, 90% of the particles have a diameter less than 31.92 μm . The MQP sample was thus composed of different size particles sizes.

3.3. Scanning Electron Microscopy (SEM)

Figure 3 presents morphological features of the composites with several MQP volume fractions, (0.01, 0.02, 0.06 and

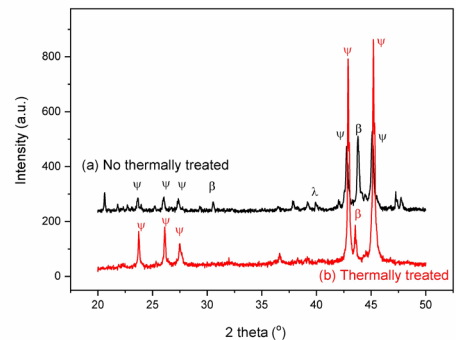


Figure 1. MQP X-ray diffraction patterns ($\lambda = K\alpha Cu = 0.154184 nm$): a) no thermally treated; b) thermally treated.

0.15). Figures 3 (a-d) reveals that for all of the composites, the MQP powder was well dispersed within the polymeric matrix. However, notable particle mix (both small and large particles), reveals the wide size distribution noted above. Due to the higher concentration of filler in the 0.15 MQP composite, the smaller particles (Figure 3f) tended to agglomerate more than in the 0.02 MQP composite (Figure 3e). The thermal behavior of polymer matrix leads to two events: a) expansion during compression molding during heating and b) contraction during cooling. Then, when the UHMWPE matrix contracts,

Table 1. Alloy elements of the AlCuFe and its respective compositions.

Elements	Composition (%)
Al	65.11
Cu	22.831
Fe	11.7773
Si (impurity)	0.2818

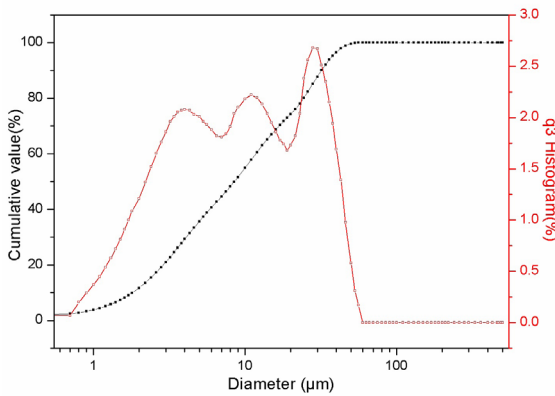


Figure 2. Particle size distribution of the MQP sample after being thermally treated for 24h.

it involves the MQP particles and consequently the filler is mechanical anchored by the matrix when the composites are subjected to fracture (Figure 3f). Contracted polymer surfaces around MPQ particles prevent them from being pulled out during fracture (Figure 3e). In the present work, neither surface treatment of the MQP nor modification of the matrix by coupling agent was used. The low MQP friction coefficient² allows processing of UHMWPE composites with higher MQP concentrations without surface treatment.

3.4. Differential Scanning Calorimetry (DSC)

Thermal characterization of the pure UHMWPE and its composites using DSC was performed establishing the melting and crystallization behavior of the samples. Table 2 provides the data obtained from the curves shown in Figure 4. Crystallization curves were obtained after the first heating and cooling from melting, as shown in Figure 4a; the width at half height of the exotherm peak (ΔW) was calculated and showed in Table 2. It can be seen that the samples have similar crystallization temperatures (T_c), confirming the weak interaction between composites constituents as shown in the morphological study. The lower value of (ΔW) of the 0.06 MQP composite indicates that its crystallite size distribution is narrower than that of the matrix, while the (ΔW) values of the other composites have no alteration. The composite melting temperatures were not altered with respect to the pure polymer, as seen in Figure 4b. The supercooling temperature ($T_m - T_c$) and ΔW were decreased, and based on other authors^{32,33} a more perfect crystallization and a narrower crystallite size distribution are thus suggested. Only the 0.06 MQP composite presented lower ($T_m - T_c$) and ΔW values when compared to UHMWPE, suggesting a trend towards a more perfect crystallization for this MQP concentration. However, the MQP additions decreased the crystallinity of the pure polymer, which presented a higher melting enthalpy than

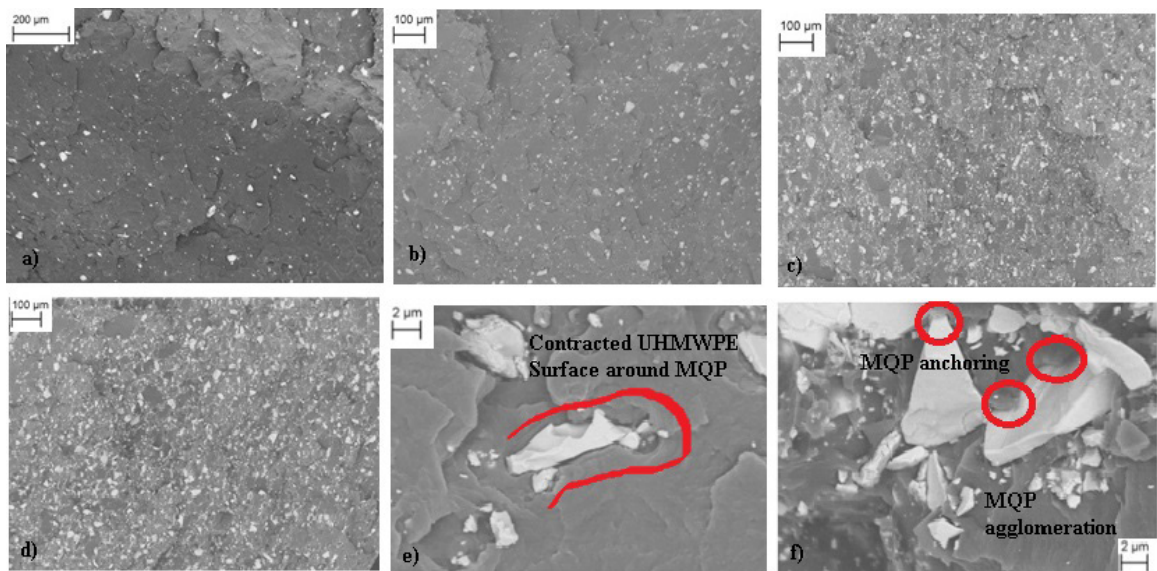
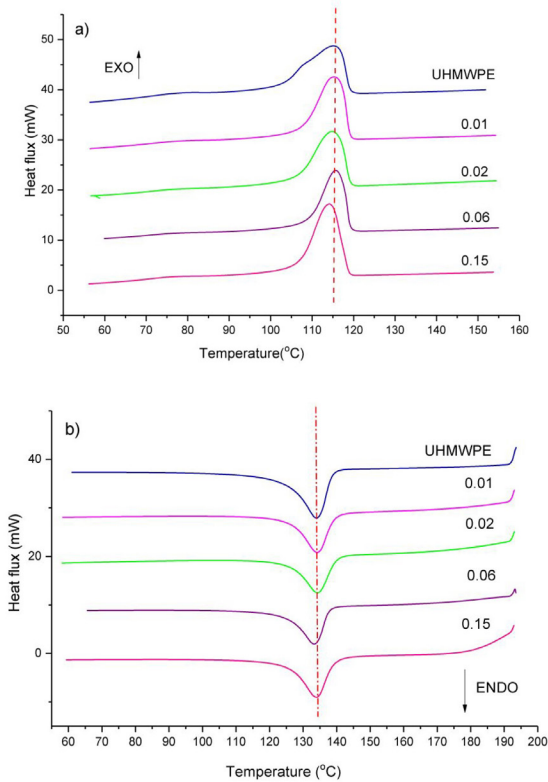


Figure 3. SEM micrographs of the composites samples: a) 0.01 MQP; b) 0.02 MQP; c) 0.06 MQP; d) 0.15 MQP; and e), f) details of the 0.02 and 0.15 MQP composites.

Table 2. DSC results for UHMWPE and its composites upon second heating.

ϕ_f	T_c (°C)	T_m (°C)	χ_c (%)	$T_m - T_c$	ΔW
UHMWPE	115.0 ± 1.9	134.1 ± 5.2	56.6 ± 2.0	19.1	9.33
0.01	115.3 ± 1.8	134.3 ± 3.9	46.6 ± 2.7	19.0	8.97
0.02	115.0 ± 2.8	134.1 ± 4.0	53.0 ± 3.1	19.1	8.01
0.06	116.1 ± 2.5	133.3 ± 3.8	50.8 ± 3.4	17.2	6.8
0.15	114.1 ± 1.6	133.7 ± 4.0	48.8 ± 4.3	19.6	9.05

**Figure 4.** DSC curves for pure UHMWPE and its composites: a) Crystallization Temperature from melting; b) Melting Temperature upon second heating.

the composites. The crystallinity of the composite with 0.15 MQP was reduced by about 16.0% compared to the pure polymer. Therefore, our results reveal that it is difficult to increase the crystallinity of UHMWPE by adding MQP, as well as when carbon nanoparticle was added, as noted by Visco et al.³⁴. Kothalkar et al.²¹ who performed thermal analysis of high density polyethylene/quasicrystalline alloy composites also observed the negative effect of Al-Ni-Co decagonal quasicrystal on polymer crystallinity. From these results, it is likely that to increase the thermal properties of UHMWPE, 0.6MQP is the more favorable composition when compared to the other composites.

3.5. Thermogravimetric Analysis (TGA)

TGA measurements indicated that with MQP addition, changes occurred in the pure UHMWPE mass loss percentage. The sample data and curves are shown in Table 3 and Figure 5, respectively. The composites presented degradation curves

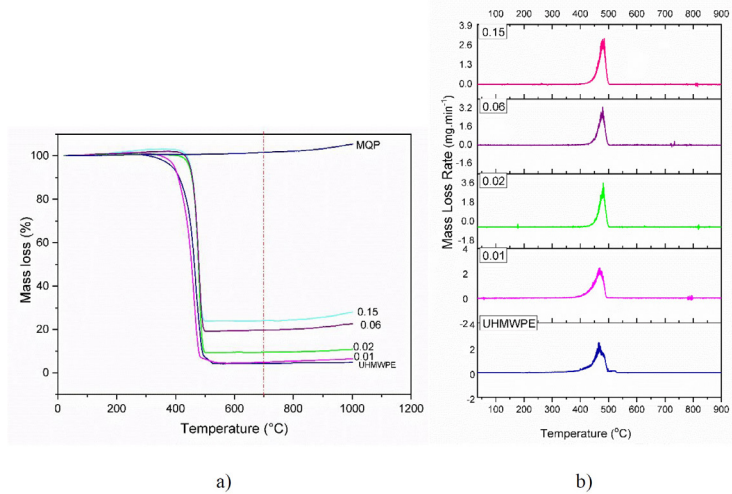
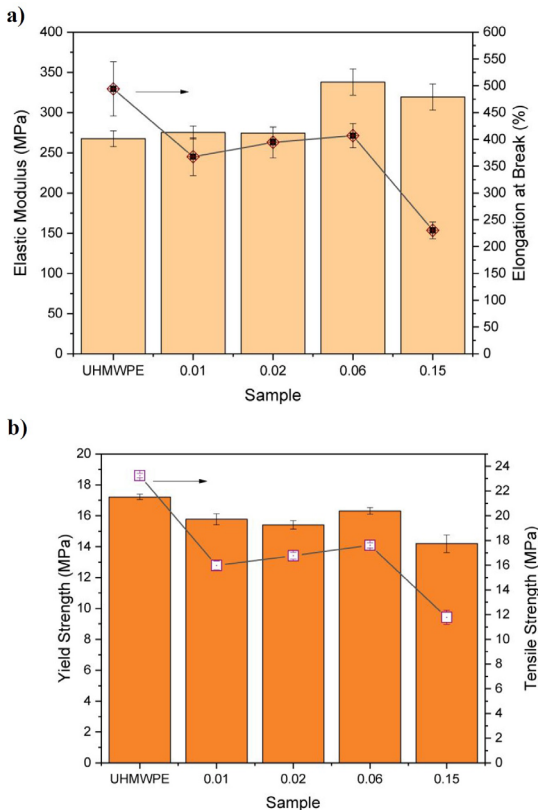
similar to that of the pure matrix with only one stage of degradation as shown in Figure. Adding MQP promoted improvement in the thermal stability of the polymer. In the case of the 0.15 MQP composite, its initial degradation temperature was 387.17 °C, and its temperature (T_{max}) at the maximum degradation rate was 490.52°C, while for UHMWPE these were respectively 260.86 and 487.38 °C. This represents improvement in these temperatures of 126.31 °C and 3.14 °C, respectively. All of the composites presented lower mass loss values than the pure matrix. When the temperatures at various mass losses (90, 80, and 50) are increased, the composites present higher temperature values than those of pure polymer, being therefore more stable, especially when the MQP addition is higher. However, when the temperatures were higher, ≈ 700 °C, the MQP and all composites presented gain of mass. From the tetragonal phase ω ($Al_{70}Cu_{20}Fe_{10}$) contained of an Al-Cu-Fe alloy, Huang et al.³⁵ using an oxidative process, obtained the Ψ -phase (quasicrystalline i-phase). This result was observed from TGA-DTA curves whose mass gain started at around 620 °C in ambient air. According to E. Huttunen-Saarivirta³⁶, the (β) phase (and other crystalline phases τ , ω and λ) may coexist with quasicrystalline phase (Ψ) due to the equilibrium conditions of peritectic reaction. These crystalline phases are more susceptible to corrosion. Thus, the presence of the crystalline phase (β) in the thermally treated sample (Figure 1b) in atmosphere without completely pure Argon may have contributed to the MQP oxidation reaction, represented by the mass gain starting at around 700 °C.

3.6. Mechanical properties

The results concerning the mechanical properties of UHMWPE and its composites are shown in Figure 6. Adding lower concentrations of MQP positively modified the Elastic Modulus (EM) of the matrix with a slight improvement. While for higher concentrations, the increase was above 20%, suggesting a matrix reinforcing effect. The composites with 0.01 and 0.02 MQP presented the same EM results as UHMWPE. For higher MQP addition, the EM values increased, mainly for the 0.06 MQP composite. According to Fu, et al.³⁷, hard particles have higher stiffness values, collaborating with improvements in the modulus of composites based in a ductile matrix, and micro and nanoparticles. The EM results of the UHMWPE/MQP composites were slightly affected by particle agglomeration; in agreement with the authors³⁸⁻⁴⁰. The yield strength (YS) of UHMWPE decreased about 17.6% with 0.15 MQP addition due to both agglomeration of small particle and large particles with small aspect ratios. For the other composites with volume fractions of 0.01 and 0.02 MQP, the YS values decreased by about 10%, while 0.06 MQP decreased around 5.0%. The YS of a composite

Table 3. TGA data of the pure UHMWPE and its composites.

ϕ_f	T _{initial} (°C)	T _{final} (°C)	T _{onset} (°C)	T _{max} (°C)	T90 (°C)	T80 (°C)	T50 (°C)	Mass Loss (%)	Residue (%)
UHMWPE	260.86	528.53	443.62	487.38	410.70	434.93	463.90	98.48	5.28
0.01	351.40	506.80	444.71	482.80	407.97	423.70	454.39	91.22	10.15
0.02	379.43	518.43	461.48	489.96	453.80	464.15	476.60	91.23	10.90
0.06	383.76	509.76	459.76	488.01	456.67	465.32	478.20	79.50	22.16
0.15	387.17	524.88	460.41	490.52	458.06	465.32	478.80	80.68	27.78

**Figure 5.** TGA curves for the samples: a) Mass Loss and b) Mass Loss Rate.**Figure 6.** Mechanical Properties for the samples: a) Elastic Modulus and Elongation at Break; b) Yield Strength and Tensile Strength.

depends on interfacial adhesion (for matrix tension to be transferred efficiently to the filler)²⁰. The yield stress and elastic modulus are also influenced by the contact area of the filler surface^{39,41}. From the EM and YS results, it is plausible to suppose that interactions between the matrix and the MQP in the 0.6 MQP composite due to the mechanical anchoring were more effective, which led to the matrix supporting greater force during the tensile testing. In respect to tensile strength (TS), it is important to consider that large particles detach from the matrix, forming large cavities in it, which result in cracks⁴². Moreover, composite strength is sensitive to changes in structure, particles size, and aggregate formation⁴¹. In fact, the reduction in TS values for all UHMWPE/MQP composites suggests the formation of cracks due to the presence of agglomerated particles. The composite with 0.15 MQP presented the worst tensile strength, which decreased about 50% compared to the pure polymer. Elongation at break (EB) of the matrix was influenced by the MQP content. All composites presented lower elongation values compared to the UHMWPE, suggesting that higher concentrations of MQP stiffen the matrix.

The expectation of interfacial interaction between MQP and UHMWPE composites motivated us to investigate it based on mathematical models. The morphological aspect of the composites evidenced the mechanical anchorage mechanism. From the "B" parameter of the Pukánszky Model, the degree of interfacial adhesion between filler and matrix can be characterized; dependent on all factors influencing the effective capacity of the cross section to support loads¹⁷. The morphological aspects of UHMWPE/MQP composites revealed smaller MQP particles, agglomeration, and interfacial

adhesion between components by mechanical anchoring, as shown in the micrographs (Figure 5e, f). Using the “B” parameter, it can be inferred which composites were less affected by the morphology, such as smaller agglomerated particles and cavities formed by the displacement of large MQP particles. Negative “B” values imply poor interfacial adhesion for the particulate composite. The “B” values for the UHMWPE/MQP composites were determined using experimental yield stress data (Table 4) and Equation 4. As shown in Table 4, negative “B” values were obtained for composites of 0.01 and 0.02 MQP. For these composites, the results indicate poor interfacial adhesion between UHMWPE and MQP as seen in the morphological aspects. Other authors^{38,39,42} are in accordance with the results obtained in the present work. The 0.06 and 0.15 MQP composites presented positive “B” value, higher than those observed for the other composites, and suggesting better interfacial adhesion for them. Remembering that the value of YS decreased less for 0.06 MQP composite, and suggest interaction between MQP and UHMWPE.

Using the Nicolais-Narkis Model, the lack of adhesion between UHMWPE and MQP was assessed: Equation 3 and $k = 1.21$. The theoretical prediction established for the UHMWPE/MQP composites is seen in Figure 7. It can be seen that the tensile yield stress values of the 0.06 and 0.15 MQP composites were above the modeling curve obtained by the Nicolais-Narkis Model²³. This suggests that there is certain interaction between components in these composites, while for the remaining composites there are lack of adhesion, because their tensile yield stress values were below the modeling curve. Yet this result was corroborated by the Pukánszky Model, which predicts quasicrystal particles in composites 0.06 and 0.15, debonding during deformation, and partial load carry applied to UHMWPE due to the positive values of B (Table 4).

Table 4. Pukánszky model “B” values for the UHMWPE/MQP composites.

ϕ_f	Parameter B
0.01	-5.26
0.02	-2.10
0.06	2.46
0.15	1.92

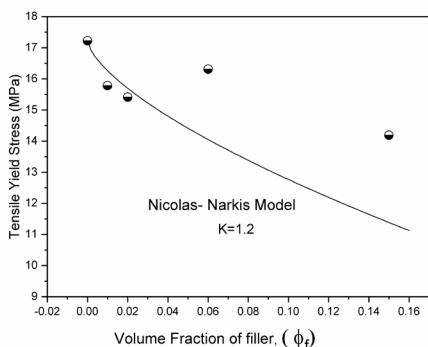


Figure 7. Tensile yield stress of the composites with Nicolais-Narkis Model theoretical prediction.

4. Conclusion

The UHMWPE crystallinity was diminished, principally for the 0.15 composite which decreased by approximately 16.0%. Morphological aspects revealed large and small MQP particles and some mechanical anchoring between particle and matrix, especially when the MQP concentration was higher. Thermal analysis revealed that addition of MQP improved thermal stability for UHMWPE in the first degradation event. However, MQP composites display an oxidative process at ≈ 700 °C, and the composites with higher concentrations of MQP presented more pronounced mass gains due to the MQP oxidation process. Stiffness (Elastic Modulus) increased for the 0.06 and 0.15 composites, while elongation at break decreased due to the reinforcing effect of the higher MQP concentrations. However, both yield and tensile strength decreased for all composites, being the 0.06 MQP composite was the least affected. The Pukánszky and Nicolais-Narkis models revealed that 0.06 and 0.15 MQP composites results, were more prone to withstand loads under tensile yield than the other composites with lower concentrations. Considering the measured stiffness and temperature resistance of the studied composites at temperatures below 500 °C, higher concentrations of MQP revealed potential as a filler for UHMWPE composites.

5. Acknowledgments

This work was supported by the Coordenação de Aperfeiçoamento de Pessoal de Nível Superior – Brasil (CAPES) – Finance Code 001. The authors are grateful to the Fast Solidification Laboratory at the Federal University of Paraíba for providing all of the characterizations.

6. References

- Souza VC, Santos EBC, Mendonça AV, Silva LB. Thermal behavior and decomposition kinetic studies of biomedical UHMWPE/vitamin C compounds. *J Therm Anal Calorim.* 2018;134:2097-105.
- Baena JC, Wu J, Peng Z. Wear Performance of UHMWPE and Reinforced UHMWPE Composites in orthoplasty Applications: a Review. *Lubricants.* 2015;3:413-36.
- Yingchun L, Hui H, Bai H, Ling Y, Peng L. In situ fabrication of cellulose nanocrystal-silica hybrids and its application in UHMWPE: rheological, thermal, and wear resistance properties. *Polym Compos.* 2018;39:E1701-13.
- Samad MA, Sinha SK. Dry sliding boundary lubrication performance of a UHMWPE/CNTs nanocomposites coating on steel substrates at elevated temperatures. *Wear.* 2011;270(5-6):395-402.
- Wang A, Essner A, Stark C, Dumbleton JH. Comparison of the size and morphology of UHMWPE wear debris produced by a hip joint simulator under serum and water lubricated conditions. *Biomaterials.* 1996;17:865-71.
- Anderson BC, Bloom PD, Baikerikar KG, Sheares VV, Mallapragada SK. AICuFe quasicrystal/ultra-high molecular weight polyethylene composites as biomaterials for acetabular cup prosthetics. *Biomaterials.* 2020;23:1761-8.
- Schwartz CJ, Bahadur S, Mallapragada SK. Effect of crosslinking and Pt–Zr quasicrystal fillers on the mechanical properties and wear resistance of UHMWPE for use in artificial joints. *Wear.* 2007;263:1072-80.

8. Bloom PD, Baikerikar KG, Anderegg JW, Sheares VV. Fabrication and wear resistance of AlCuFe quasicrystal-epoxy composite materials. *Mater Sci Eng A*. 2003;360:46-57.
9. Niu Y, Zheng S, Song P, Zang X, Wang C. Mechanical and thermal properties of PEEK composites by incorporating inorganic particles modified phosphates. *Compos, Part B Eng*. 2021;212:108715.
10. Sakly A, Kenzari S, Bonina D, Corbel S., Fournée V. A novel quasicrystal-resin composite for stereolithography. *Mater Des*. 2014;56:280-5.
11. Shechtman D, Blech I, Gratias D, Cahn JW. Metallic phase with long-range orientational order and no translational symmetry. *Phys Rev Lett*. 1984;53:1951-3.
12. Levine D, Steinhardt PJ. Quasicrystals: A new class of ordered structures. *Phys Rev Lett*. 1984;53:2477-80.
13. Yadav TP, Mukhopadhyay NK. Quasicrystal: a low frictional novel material. *Curr Opin Chem Eng*. 2018;19:163-9.
14. Dubois JM, Belin-Ferré E. Wetting and adhesion properties of quasicrystals and complex metallic alloys. *Appl Adhes Sci*. 2015;3:1-16.
15. Dubois JM. Properties—and applications of quasicrystals and complex metallic alloys. *Chem Soc Rev*. 2012;41:6760-77.
16. Tsai AP, Aoki K, Inoue A, Masumoto T. Synthesis of stable quasicrystalline particle-dispersed Al base composite alloys. *J Mater Res*. 1993;8:5-7.
17. Pukánszky B. Influence of interface interaction on the ultimate tensile properties of polymer composites. *Composites*. 1990;21:255-62.
18. Móczó J, Fekete E, László K, Pukánszky B. Aggregation of particulated filler: factors, determination, properties. *Macromol Symp*. 2003;194:111-24.
19. Melo PMA, Macêdo OB, Barbosa GP, Santos ASF, Silva LB. Reuse of natural waste to improve the thermal stability, stiffness, and toughness of postconsumer polypropylene composites. *J Polym Environ*. 2021;29:538-51.
20. Müllera P, Renner K, Móczó J, Fekete E, Pukánszky B. Thermoplastic starch/wood composites: interfacial interactions and functional properties. *Carbohydr Polym*. 2014;102:821-9.
21. Kothalkar A, Sharma AS, Tripathi G, Basu B, Biswas K. HDPE-quasicrystal composite: fabrication and wear resistance. *Trans Indian Inst Met*. 2012;65:13-20.
22. Fernandes MRP, França TS, Queiroz IX, Wanderley WF, Cavalcante DGL, Passos TA, et al. Insights of PHB/QC biocomposites: thermal, tensile and morphological properties. *J Polym Environ*. 2020;28:2481-9.
23. Nicolais L, Nicodemo L. Strength of particulate composite. *Polym Eng Sci*. 1973;13:469-77.
24. Krevelen DW. *Properties of polymers*, Amsterdam: Elsevier Sciences Publishers; 1990.
25. Passos TA, Gomes RM, Melo TA, Lima SJG. Investigation of quasicrystal-Reinforced Aluminium Metal Matrix composite by hot extrusion. *Mater Sci Forum*. 2010;643:125-9.
26. Pukánszky B, Todos F, Jancar J, Kolarik J. The possible mechanisms of polymer-filler interaction in polypropylene-CaCO₃ composites. *J Mater Sci Lett*. 1989;8:1040-2.
27. Renner K, Yang MS, Móczó J, Choi HJ, Pukánszky B. Analysis of the debonding process in polypropylene model composites. *Eur Polym J*. 2005;41:2520-9.
28. Dubois JM, Belin-Ferré E, Feuerbacher M. Introduction to the science of complex metallic alloys. basic of thermodynamics and phase transition in complex intermetallics. Vol. 1. Paris: World Scientific Publishing; 2008.
29. Dubois JM. *Useful quasicrystals*. Singapore: World Scientific Publishing; 2005.
30. Srinivas V, Barua P, Murty BS. On icosahedral phase formation in mechanically alloyed Al70Cu20Fe10. *Mater Sci Eng*. 2000;294-296:65-7.
31. Barua P, Srinivas V, Murty BS. Synthesis of quasicrystalline phase by mechanical alloying of Al70Cu20Fe10. *Philos Mag A Phys Condens Matter Struct Defects Mech Prop*. 2000;80:1207-17.
32. Sun P, Qian TY, Ji XY, Wu C, Yan YS, Qi RR. HDPE/UHMWPE composite foams prepared by compression molding with optimized foaming capacity and mechanical properties. *J Appl Polym Sci*. 2018;135:46768.
33. Sui G, Zhong WH, Ren X, Wang XQ, Yang XP. Structure, mechanical properties and friction behavior of UHMWPE/HDPE/carbon nanofibers. *Mater Chem Phys*. 2009;115:404-12.
34. Visco A, Yousef S, Galtieri G, Nocita D, Pistone A, Njuguna J. Thermal, mechanical and rheological behaviors of nanocomposites based on UHMWPE/paraffin oil/carbon nanofiller obtained by using different dispersion techniques. *JOM*. 2016;68:1078-89.
35. Huang JR, Yamane H, Tsai AP. Fabrication of Al-Cu-Fe particles containing quasicrystalline ω -phase by oxidation of ω -phase in air. *J Mater Sci*. 2020;55:12448-57.
36. Huttunen-Saarivirta E. Microstructure, fabrication and properties of quasicrystalline Al-Cu-Fe alloys: a review. *J Alloys Compd*. 2004;363:154-78.
37. Fu SY, Feng XQ, Lauke B, Mai YW. Effects of particle size, particle/matrix interface adhesion and particle loading on mechanical properties of particulate polymer composites. *Compos, Part B Eng*. 2008;39:933-61.
38. Százdí L, Pukánszky B Jr, Vancso GJ, Pukánszky B. Quantitative estimation of the reinforcing effect of layered silicates in PP nanocomposites. *Polymer*. 2006;47:4638-48.
39. Pukánszky B, Fekete E. Aggregation tendency of particulate fillers: determination and consequences. *Period Polytech Chem Eng*. 1998;42:167-86.
40. Móczó J, Fekete E, László K, Pukánszky B. Aggregation of particulate fillers: factors, determination, properties. *Macromol Symp*. 2003;104:111-24.
41. Metin D, Tihminlioglu F, Balkose D, Ulku S. The effect of interfacial interactions on the mechanical properties of polypropylene/natural zeolite composites. *Compos - A Appl Sci Manuf*. 2004;35(1):23-32.
42. Renner K, Kenyó C, Móczó J, Pukánszky B. Micromechanical deformation processes in PP/wood composites: particle characteristics, adhesion, mechanisms. *Compos Part A-Appl S*. 2010;41:1653-61.